

Investigating Neoproterozoic Sedimentary Successions in Siberia and British Columbia using Re-Os Geochronology

Evelyn Larson

Advisor: Alan Rooney

Second Reader: Jordan Wostbrock

May, 2023

A Senior Thesis presented to the faculty of the Department of Earth and Planetary Sciences, Yale University, in partial fulfillment of the Bachelor's Degree.

In presenting this thesis in partial fulfillment of the Bachelor's Degree from the Department of Geology and Geophysics, Yale University, I agree that the department may make copies or post it on the departmental website so that others may better understand the undergraduate research of the department. I further agree that extensive copying of this thesis is allowable only for scholarly purposes. It is understood, however, that any copying of publication of this thesis for commercial purposes or financial gain is not allowed without my written consent.

Evelyn Larson

May, 2023

Table of Contents

1. Abstract	2
2. Introduction	3
3. Background	4
3.1 Carbon Isotope Chemostratigraphy	4
3.2 Re-Os Geochronology	6
4. Geologic Context	8
4.1 Patom Supergroup, Central Siberia, Russia	8
4.2 Taseeva Group, Southwestern Siberian Platform, Russia	11
4.3 Windermere Supergroup, British Columbia, Canada	14
5. Methodology	20
5.1 Sample Preparation	20
5.2 Rhenium Tests	20
5.3 Re-Os Analysis	21
6. Results	23
6.1 Rhenium Abundance	23
6.1.1 Patom Supergroup	23
6.1.2 Imbinskaya Well Core	23
6.1.3 Windermere Supergroup	24
6.2 Re-Os Isotopic Analysis	25
6.2.1 Imbinskaya Well Core	25
6.2.2 Windermere Supergroup	25
7. Discussion	27
7.1 Patom Supergroup	27
7.2 Taseeva Group	27
7.3 Windermere Supergroup	28
8. Conclusions and Future Work	29
9. Acknowledgments	30
10. References	30

1. Abstract

The Neoproterozoic Era (1000 Ma - 539 Ma) recorded dramatic fluctuations in Earth systems, including Snowball Earth glaciations, increasing oxygenation of the ocean, radiation of metazoans, rapid plate motions, and major perturbations to global biogeochemical cycles. Near the close of the Neoproterozoic, Snowball Earth events and the Shuram carbon isotope excursion recorded some of the largest of these perturbations. The Shuram has been recognized globally, although poor age constraints in multiple locations have led to significant controversy over the excursion's timing, duration, and drivers, as well as its role in coincident environmental and ecological developments. Geochronology is the key to unraveling the relationships between the Neoproterozoic geochemical record and global events. This study seeks to constrain the timing of Snowball Earth glaciations and the Shuram excursion in Neoproterozoic deposits on the margin of the Siberian craton and in southwestern Canada using the Re-Os radiogenic isotope system.

2. Introduction

The Neoproterozoic Era (1000 Ma-539 Ma) was a dynamic period of Earth's history, characterized by dramatic variations in climate, ocean-chemistry fluctuations, and biological diversification. This era is divided into the Tonian (1000 Ma - 720 Ma), Cryogenian (720 Ma - 635 Ma), and Ediacaran (635 Ma - 539 Ma) periods. The Cryogenian period is marked by two global Snowball Earth events, the Sturtian and the Marinoan, during which the entirety of Earth's surface was glaciated (Kirschvink 1992; Hoffman et al. 2017; Kaufman, Knoll, and Narbonne 1997). After each major glaciation, the carbon isotopic signature of the ocean temporarily dropped as recorded in overlying cap carbonates, causing negative $\delta^{13}\text{C}$ excursions (Knoll et al. 1986; Narbonne et al. 2012). The carbon isotope record was subsequently driven to its lowest known values during the Ediacaran Shuram excursion (Grotzinger, Fike, and Fischer 2011). By the late Ediacaran, the Earth's surface had become increasingly oxic, which possibly facilitated the appearance and radiation of new and complex life forms (Fike et al. 2006; Erwin et al. 2011). Tectonic activity and rapid plate motion, including the breakup of Rodinia and assembly of Gondwana, may have contributed to the major biogeochemical changes that took place during the Neoproterozoic (Meert and Lieberman 2008). The Neoproterozoic is an enigmatic era, but nevertheless crucial for understanding the development of the geochemical and biological regimes that govern Earth's systems.

This study seeks to use the Re-Os geochronology system to refine age models for Ediacaran stratigraphy in two locations on the margin of the Siberian craton and in the Windermere Supergroup of British Columbia, Canada. These strata exhibit Shuram-correlated carbon isotope excursions and lithostratigraphic evidence of Snowball Earth glaciations, but lack definitive radioisotope age constraints. Work was first done on the Patom Supergroup in south central Siberia, though the samples turned out to be unsuitable for Re-Os analysis. Drillcores from the Taseeva Group of southwest Siberia were also investigated, although with a lack of stratigraphic information and the development of geopolitical events. However, we recently shifted attention to the Windermere Supergroup, for which Re-Os analysis is ongoing. Altogether, the three locations represent promising opportunities to further define and constrain important geobiological events during the Neoproterozoic Era.

3. Background

3.1 Carbon Isotope Chemostratigraphy

Due to the low resolution of biostratigraphy during the Neoproterozoic, chemostratigraphy and geochronology are the main tools used to refine the stratigraphy of the era. In particular, the carbon isotope record gives insight into concurrent perturbations to the carbon cycle within local and global stratigraphic frameworks. The two most stable carbon isotopes are ^{12}C and ^{13}C , and the ratio between them can be expressed in delta notation,

$$\delta^{13}\text{C} = \left(\frac{\left(\frac{^{13}\text{C}}{^{12}\text{C}} \right)_{\text{sample}}}{\left(\frac{^{13}\text{C}}{^{12}\text{C}} \right)_{\text{standard}}} - 1 \right) \times 1000 \text{‰} \quad \text{Eq. 1}$$

where the ratio of $^{13}\text{C}/^{12}\text{C}$ of the sample is normalized to the $^{13}\text{C}/^{12}\text{C}$ ratio of the Vienna Pee Dee Belemnite standard. A negative, or light, $\delta^{13}\text{C}$ value indicates an over abundance of ^{12}C compared to the standard, and a positive, or heavy, $\delta^{13}\text{C}$ value indicates an over abundance of ^{13}C . In steady state, the carbon cycle and $\delta^{13}\text{C}$ of carbonates are primarily regulated by primary productivity and organic carbon burial efficiency.

The two largest surface reservoirs of carbon are marine dissolved organic carbon (DOC) and dissolved inorganic carbon (DIC). While photosynthetic processes preferentially uptake ^{12}C and thus strongly enrich the DOC in ^{12}C ($\delta^{13}\text{C}_{\text{org}} = -20\text{‰}$ to -30‰), the DIC reservoir is much larger and has a less negative $\delta^{13}\text{C}_{\text{carb}}$ value. Over geologic timescales, the $\delta^{13}\text{C}_{\text{org}}$ and $\delta^{13}\text{C}_{\text{carb}}$ values of seawater should balance to $\sim -6\text{‰}$ (Schidlowski and Aharon 1992). Isotopic fractionation during the precipitation of carbonate is negligible, so carbonates tend to record the sea water $\delta^{13}\text{C}$ value at the time of deposition. While the carbonate record has been primarily steady at 0‰ through geologic time, it also records imbalances in the biogeochemical carbon cycle in the form of positive (high $\delta^{13}\text{C}_{\text{carb}}$) and negative (low $\delta^{13}\text{C}_{\text{carb}}$) carbon isotope excursions (CIEs) (Saltzman and Thomas 2012; Grotzinger, Fike, and Fischer 2011; Knoll et al. 1986).

Some of the most dramatic of these excursions occur during the Neoproterozoic, which are used to date and correlate strata globally. For example, the distinct cap carbonates that overlie the glacial diamictites of the Sturtian and Marinoan Snowball Earth events exhibit negative CIEs with a nadir of $\sim -5\%$ (Halverson et al. 2005). Cap carbonate negative excursions have been interpreted as a sign of suppressed primary productivity and low burial rates of organic material following glaciation (Schidlowski and Aharon 1992). Since carbonates are precipitated in warm, shallow water, their precipitation following major glacial events indicates that the global ocean warmed quickly at the termination of Snowball Earth events. Additionally, Snowball Earth cap carbonates are characterized globally by unusual sedimentary textures, including mega-ripples, aragonite and barite crystal fans, tubelike structures, and seafloor cements (Halverson et al. 2005; James, Narbonne, and Kurtis Kyser 2001). The combination of carbon isotope stratigraphy and independent, unique stratigraphic evidence allows for global correlation of the Snowball Earth cap carbonates, although precise radiometric ages are not available for many of these formations.

The Ediacaran Shuram excursion is the largest negative CIE in geologic history. It marks a sharp decrease in $\delta^{13}\text{C}$ to values with a nadir of about -12% , before a slow recovery over the course of millions of years (fig. 1B) (Grotzinger, Fike, and Fischer 2011). This carbon isotope trend is very distinct in both magnitude and duration, and has been observed globally, including in Oman, Australia, China, and Death Valley (fig. 1A). Unlike those of the Snowball Earth cap carbonates, sedimentary features of Shuram-associated formations are usual, representing shallow mixed carbonate-siliciclastic marine environments. Some formations have deeply-incised submarine canyons cutting through the isotope excursion strata (Grotzinger, Fike, and Fischer 2011; Busch et al. 2022). Significant controversy exists over the causes of the Shuram excursion, with the main models arguing either for a primary or a diagenetic cause (Grotzinger, Fike, and Fischer 2011, and references therein). The Shuram CIE has been shown to be synchronous in at least two separate paleocontinents, with its onset and termination at 574.0 ± 4.7 and 567.3 ± 3.0 Ma (Rooney et al. 2020), though most Shuram-bearing strata lack precise age constraints (fig. 1A). Thus, constraining the onset and termination in as many localities as possible may give insights into its possible driving mechanisms.

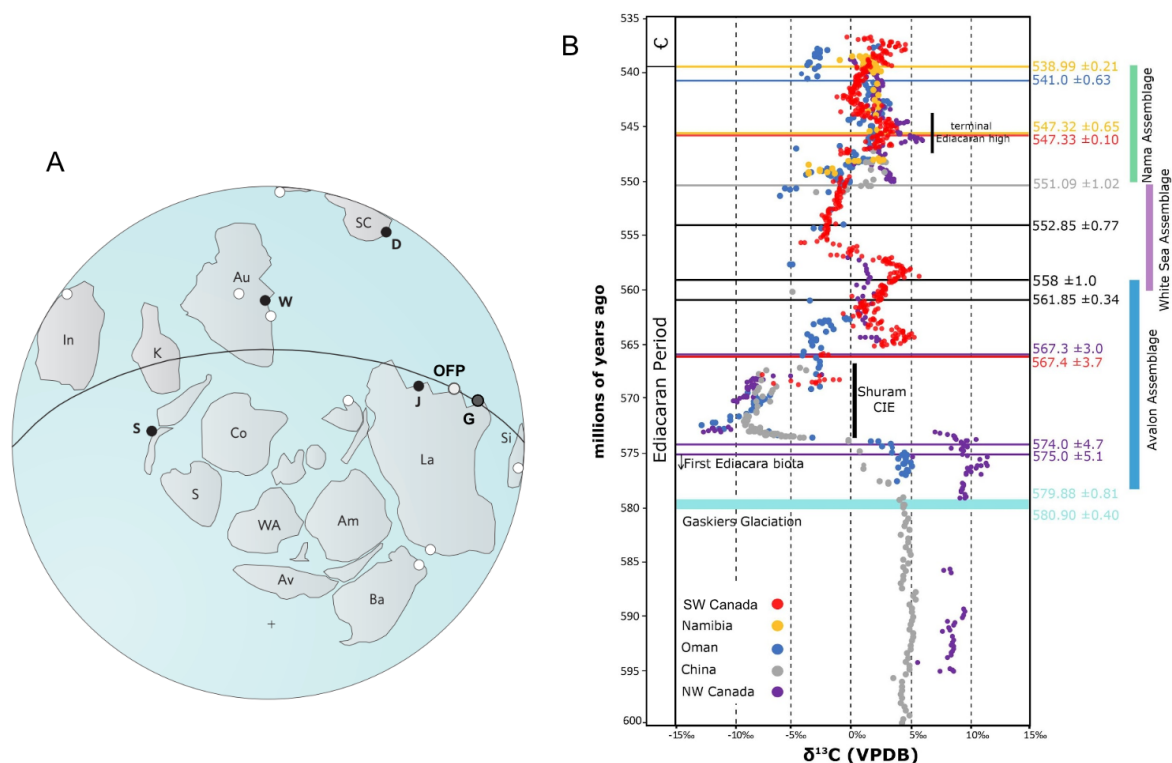


Figure 1. (A) Paleogeographic map (600 Ma) with global distribution of the Shuram CIE. Key sections for the Shuram are indicated by filled circles (S, Shuram; W, Wonoka; D, Doushantuo; J, Johnnie; G, Gametrail), and the position of other potential sections that may correlate with the Shuram are shown as open circles (OFF, Old Fort Point. Am, Amazonia; Au, Australia; Av, Avalonia; Ba, Baltica; Co, Congo; I, India; K, Kalahari; La, Laurentia; S, Sahara; Si, Siberia; SC, South China; WA, Western Australia. Adapted from Grotzinger et al., 2011. (B) Compilation of carbonate $\delta^{13}\text{C}$ data from basins around the world spanning 600-535 Ma, highlighting the magnitude and duration of the Shuram. Adapted from Boag et al., 2020.

3.2 Re-Os Geochronology

The two naturally occurring isotopes of rhenium are stable ^{185}Re and radioactive ^{187}Re , which decays with a half life of ~ 41.6 billion years to ^{187}Os . The Re-Os system has multiple uses, including as a method for investigating high-temperature magmatic processes, formation of ore deposits, and continental crustal evolution, and as a proxy for studying weathering and changes in seawater chemistry (Shirey and Walker 1998; B. Peucker-Ehrenbrink and Ravizza 2000). The use of the Re-Os radiogenic isotope system as a geochronometer for organic-rich sedimentary rocks was pioneered in the late 1980s (Ravizza and Turekian 1989), and has since been greatly improved by significant advances in sample digestion and analytical methods over the years (Cohen et al. 1999; Robert A Creaser et al. 2002). High precision Re-Os analysis is carried out

using isotope dilution and negative thermal ionization mass spectrometry (R. A. Creaser, Papanastassiou, and Wasserburg 1991). Using the isochron dating method, the $^{187}\text{Os}/^{188}\text{Os}$ ratio is plotted against $^{187}\text{Re}/^{188}\text{Os}$ (fig. 2). ^{188}Os is used to normalize the radiogenic component, as it is stable and has a fixed planetary abundance. An isochron (fig. 2) is defined by the following equation:

$$\left(\frac{^{187}\text{Os}}{^{188}\text{Os}}\right)_{\text{present}} = \left(\frac{^{187}\text{Os}}{^{188}\text{Os}}\right)_{\text{initial}} + \left(\frac{^{187}\text{Re}}{^{188}\text{Os}}\right) \cdot (e^{\lambda t} - 1),$$

Eq. 2

where λ is the decay constant of ^{187}Re , time since deposition (t) is proportional to the slope of the isochron, and the intercept gives the initial $^{187}\text{Os}/^{188}\text{Os}$ ratio at the time of deposition. Re and Os in organic-rich sediments are primarily sequestered from seawater at the time the sediment is deposited (Selby and Creaser 2003). In order to retain this primary record, rocks must be sheltered from significant surficial weathering, as Re and Os are mobile in weathering processes (Bernhard Peucker-Ehrenbrink and Hannigan 2000).

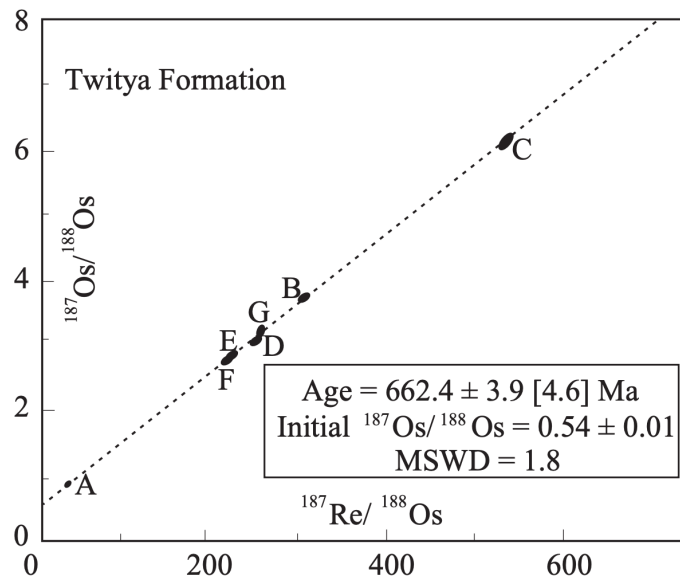


Figure 2. Example of a Re-Os isochron, where the slope of the line defined by the system is proportional to the age of the system, and the y-intercept of the line gives the initial $^{187}\text{Os}/^{188}\text{Os}$ isotopic composition at the time of deposition. From (Rooney et al. 2014).

4. Geologic Context

4.1 Patom Supergroup, Central Siberia, Russia

The Neoproterozoic Patom Supergroup is exposed in the Baikal-Patom Highland along the southern margin of the Siberian platform. The Ura uplift section of the Patom Basin is well preserved and has not undergone extensive metamorphism (fig. 3) (Chumakov et al. 2011; Chumakov, Semikhatov, and Sergeev 2013). The Patom Supergroup consists of a ~4 km thick sequence of carbonate-terrigenous sediments of the groups Ballagannakh, Dal'nyaya Taiga, Zhuya, and Trehversta (fig. 4). This sequence was deposited in a basin confined to the margin of the Siberian Craton associated with the breakup of Rodinia (Metelkin, Vernikovskiy, and Kazansky 2012; Powerman et al. 2015). The Patom Supergroup preserves records of climatic changes, ocean chemistry cycling, and biological diversification and is therefore a key section for studying the progression of climate and biological evolution during the late Neoproterozoic.

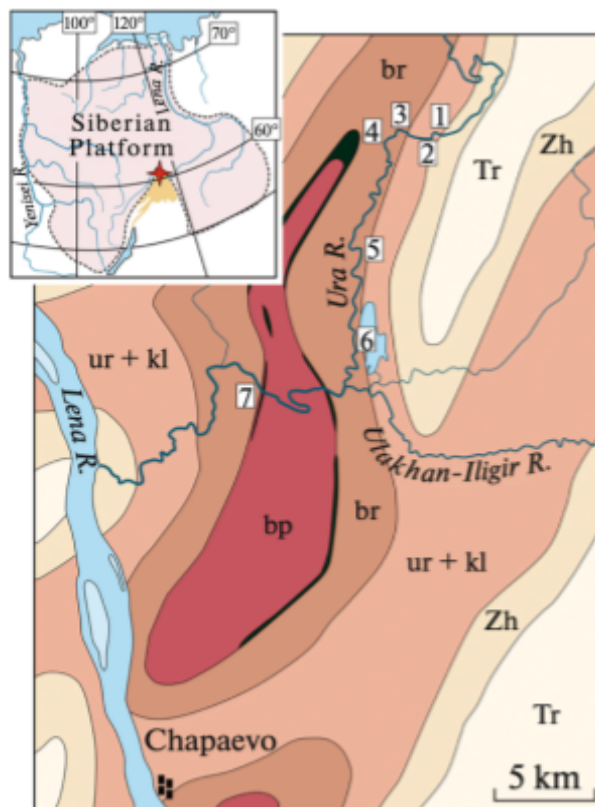


Figure 3. Location and geological structure of the Ura Uplift section of the Patom Basin (Chumakov et al., 2013) and location of the studied sections in the Ura anticline. Groups: (Zh) Zhuya, (Tr) Trehversta. Formations: (bp) Bol'shoi Patom, (br) Barakun, (ur) Ura, (kl) Kalancha. From Petrov and Pokrovsky, 2020.

The largest group, Dal'nyaya Taiga, is divided into four Formations: Bol'shoi Patom, Barakun, Ura, and Kalancha (fig. 4). The 900-1100 m thick Bol'shoi Patom Formation consists mainly of massive and bedded glacial diamictites and has been chemostratigraphically correlated with the end-Cryogenian Marinoan Glaciation (Chumakov et al. 2011). The lower contact of the Bol'shoi Patom Formation has not been observed, but it is assumed to rest conformably on the Mariinsky Formation, since it includes breccias with clasts lithologically similar to the Mariinsky limestone (Chumakov, Semikhatov, and Sergeev 2013). The base of Barakun Formation rests on the Bol'shoi Patom Formation and contains a cap dolostone with sedimentary structures and isotopic records that correlate with global Marinoan cap carbonate features (Pokrovsky et al. 2010). The cap carbonate is overlain by a 100-120 m thick section of sandstone overlain by alternating members of dark limestone and black shale (Chumakov, Semikhatov, and Sergeev 2013; Rud'ko et al. 2021).

Atop the Barakun Formation lies the Ura Formation, a 700-900 m package of thick silty mudstones with intercalated carbonates. Early Ediacaran acanthomorphic palynoflora (ECAP) occur in several horizons within both the upper Barakun and the upper Ura Formations (Chumakov, Semikhatov, and Sergeev 2013; Vorob'eva and Petrov 2020). The Kalancha Formation is the uppermost of the Dal'nyaya Taiga Group and consists of ~400 m of black to dark grey limestone and dolostone (Chumakov, Semikhatov, and Sergeev 2013). Significant changes in detrital zircon ages suggest a stratigraphic unconformity at the base of the overlying Zhuya Group (Powerman et al. 2015). The amplitude of the negative carbon isotope excursion found in the Zhuya matches that of the Shuram excursion, which, along with $^{87}\text{Sr}/^{86}\text{Sr}$ values of the Zhuya group carbonate rocks, suggests a correlation with global counterparts of the Shuram excursion (Pokrovsky, Melezhik, and Bujakaite 2006; Melezhik 2009).

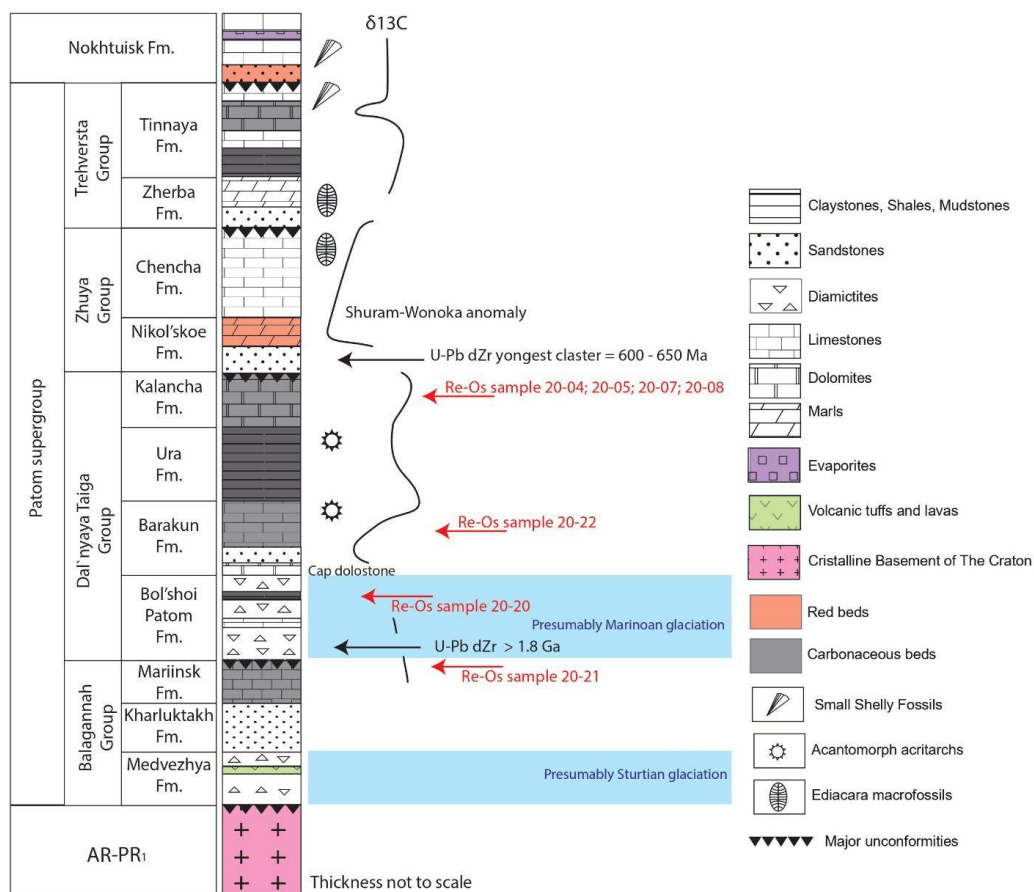


Figure 4. Stratigraphic column for the Ura Uplift section of the Patom Basin. Stratigraphic position of Re-Os samples from this study are marked in red. Current geochronological constraints are marked in black. The Cryogenian-Ediacaran boundary is presumably located at the base of the Barakun Formation.

Although chemostratigraphic and biostratigraphic markers within the Patom Supergroup have been investigated and globally correlated, attempts to constrain formation ages have yielded conflicting results with large uncertainties. Detrital zircons from the base of the Zhuya Group indicate a maximum depositional age of about 647 ± 3 Ma (Chumakov et al. 2011). However, chemostratigraphic data from the Zhuya Group indicate that its base should have a significantly younger age allied with the onset of the Shuram excursion at ~ 580 Ma (Rooney et al. 2020). Ages within the Dal'nyaya Taiga Group are defined by Pb-Pb isochron dating of limestones from the Barakun and Kalancha Formations, which yielded depositional ages of 613 ± 56 Ma (lower Barakun), 581 ± 16 Ma (upper Barakun), and 574 ± 20 Ma (upper Kalancha). Despite large uncertainties, these geochronological constraints confirm an Ediacaran age for the Dal'nyaya Taiga Group (Rud'ko et al. 2021).

Rocks from the Mariinsky, Bol'shoi Patom, Barakun, and Kalancha Formations were sent to the Rooney Geochronology Lab for Re-Os isotopic analysis. These samples consist of dark grey limestone with pyrite inclusions, thinly laminated black shale, dark grey limestone, dark grey argillite, dark grey aragonite crystal fans, and ooid, oncoid dark gray limestone (fig. 4). Re-Os age constraints on these horizons would prove valuable in correlating bio- and chemostratigraphic features of the Patom Supergroup with the global temporal framework of the late Neoproterozoic.

4.2 Taseeva Group, Southwestern Siberian Platform, Russia

The Ediacaran Taseeva Group outcrops along the southwestern margin of the Siberian craton across the Yenisei Ridge region, which has been extensively drilled in the course of oil and gas exploration. Although the Taseeva Group is exposed mainly along the eastern margin of the southern Yenisei Ridge, the group can be traced through well cores as far as 150 km east of the Yenisei Ridge (fig. 5B) (Kochnev et al. 2020). The Taseeva Group consists of a ~3 km thick sedimentary sequence of the Aleshina, Chistyakova, and Moshakova Formations (fig. 5A). This sequence includes red sandstones and siltstones with interbedded dark mudstones and carbonates, which were deposited within a foredeep basin on the southern margin of the Siberian craton (Sobolev et al. 2015; Priyatkina et al. 2018; Kochnev et al. 2020). Limited geochronologic, biostratigraphic, and chemostratigraphic constraints on the Taseeva Group stratigraphy allow tentative correlation with other groups on the margin of the Siberian craton.

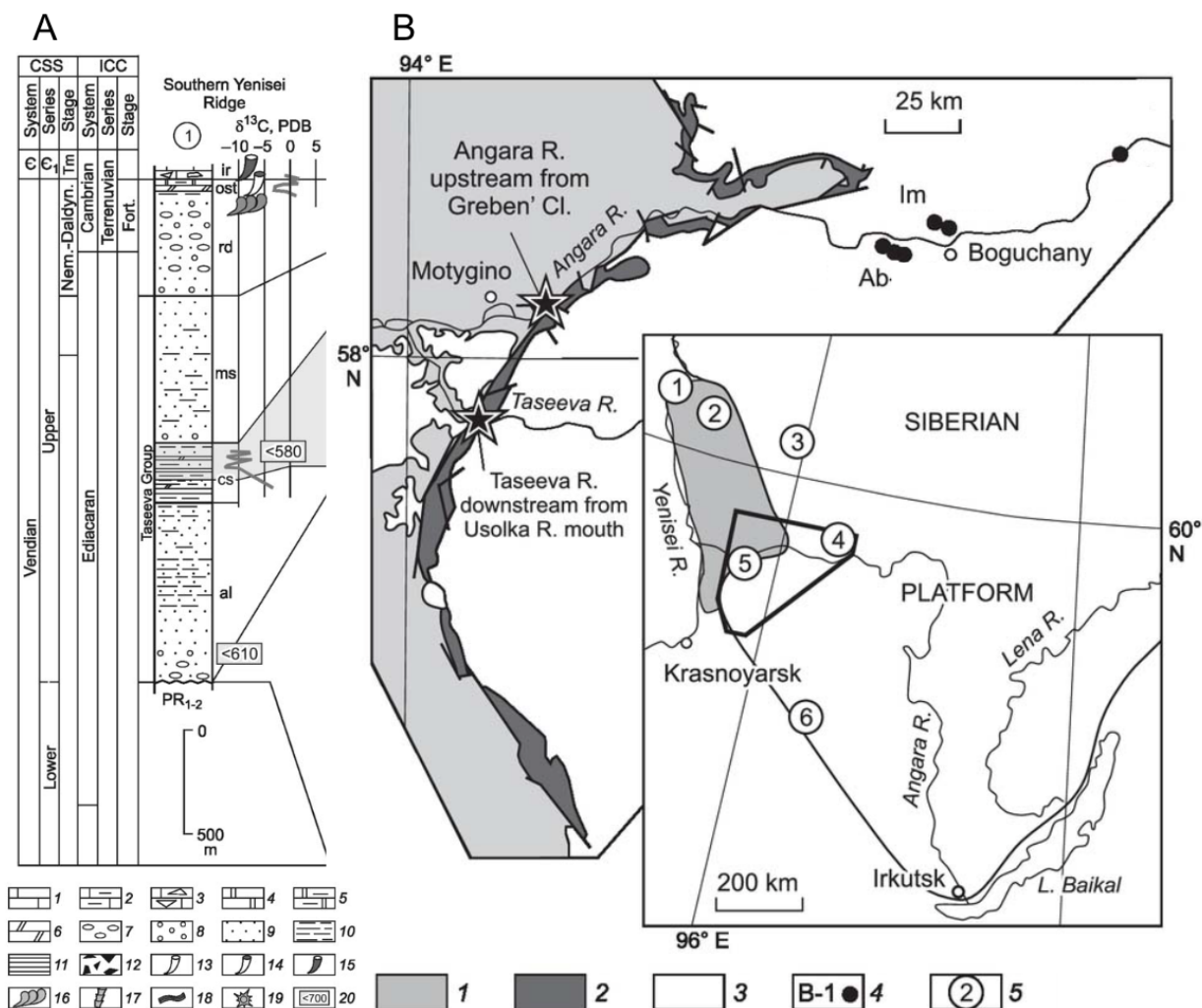


Figure 5. (A) Chemostratigraphic data for the Ediacaran Taseeva Group of the Southern Yenisei Ridge. The Shuram C-isotope anomaly analogue is highlighted in grey. 1, limestones; 2, clayey limestones; 3, limestone breccias; 4, dolostones; 5, clayey dolostones; 6, dolomite marls; 7, conglomerates; 8, gravelstones; 9, sandstones; 10, siltstones; 11, mudstones; 12, diamictites; 13–15, small shelly fossils; 16, ichnofossils *Treptichnus pedum*; 17, skeletal fossils *Namacalathus* sp.; 18, macroalgae *Vendotaenia*; 19, Ediacaran acanthomorphic microfossils; 20, minimum depositional ages by detrital zircons: Kochnev et al., 2020 and Priyatkina et al., 2018. Abbreviated formation names: ir, Irkineeva; ost, Ostrovnoy, rd, Redkolesny; ms, Moshakova; cs, Chistyakova; al, Aleshina. (B) Distribution of the Taseeva Group south of the Yenisei Ridge, and location of Neoproterozoic sequences at the southwestern margin of the Siberian Platform. 1, Proterozoic sequences of Yenisei Ridge; 2, Ediacaran deposits of Taseeva Group; 3, Phanerozoic cover of the Siberian Platform; 4, deep drilling areas into Taseeva Group deposits, including: Ab, Abakanskaya; Im, Imbinskaya; The Taimbinskaya drilling area is located nearly 200 km to the northeast of this region; 5, notable Ediacaran sediment localities. From Kochnev et al., 2020.

The Aleshina Formation and the Moshakova Formation incorporate interbedded red sandstone and siltstone with gravelite and conglomerates near the base of each section (Priyatkina et al.

2018; Kochnev et al. 2020) The Chistyakova Formation lies conformably between the two, and includes grey sandstones and siltstones, along with interbedded dark mudstones and few dolomites and dolomite marls (Kochnev et al. 2020). An erosional unconformity separates the top of the Moshakova Formation from the overlying red beds of the Redkolesny Formation.

Limited chemostratigraphic work on the Chistyakova Formation suggests that the upper half of the formation is a Shuram Excursion correlative, with carbon isotope values of -7‰ to -13‰ (Kochnev et al. 2020). A correlation between the Chistyakova Formation, the Zhuya Formation of the Patom Basin, and other Ediacaran sections of the southern margin of the Siberian craton has been recognized (Kochnev et al. 2020). Additionally, detrital zircons from the uppermost part of the Chistyakova Formation yield a maximum depositional age of about 580.0 ± 9.1 Ma (Kochnev et al. 2020)), consistent with current geochronology for the Shuram Excursion (Rooney et al. 2020). A single detrital zircon at the base of the Aleshina Formation yields an age of ~610 Ma, though the maximum depositional age determined in the same study is 1804 ± 20 Ma (Priyatkina et al. 2018). Microfossils have been found within the Aleshino and Chistyakova Formations, but all of the taxa are found within rocks from Mesoproterozoic to Cambrian in age, and are therefore not suitable for use in biostratigraphic correlations (Liu et al. 2013). Fossils from the overlying Redkolesny Formation indicate that it might straddle the Ediacaran-Cambrian transition, with an age between 542–534 Ma (Liu et al. 2013; Priyatkina et al. 2018).

Numerous drill cores within the Yenisei Ridge region sample Cambrian and Neoproterozoic deposits to a depth of about 3000 m for use in oil and gas exploration. Sections of three of these drill cores were shipped to the Rooney Geochronology Lab, including the Taimbinskaya 1, Abakanskaya 2, and Imbinskaya 3 wells. We began work on the Imbinskaya 3 well core. Based on lithology, the material studied is assumed to come from the Chistyakova Formation at a depth of about 2500 m, though detailed stratigraphic information is not available (Sobolev et al. 2015). Re-Os age constraints on well core samples from the Yenisei Ridge region would allow more precise correlation between the Taseeva Group and similar groups found along the margin of the Siberian craton.

4.3 Windermere Supergroup, British Columbia, Canada

Rocks of the Windermere Supergroup form a narrow belt from Alaska to Mexico and preserve a Neoproterozoic passive margin associated with the rifting of the supercontinent Rodinia. In the southern Canadian Cordillera, the Windermere Supergroup consists of a ~9 km thick sedimentary succession of mixed siliciclastics with some carbonates and rare mafic volcanic rocks (figs. 6, 7) (Gerald M. Ross, Bloch, and Krouse 1995). Deposition of the Windermere Supergroup occurred in two phases. The first phase was synchronous with rifting, while the second deposited an extensive deep-marine turbidite system (Gerald M. Ross, Bloch, and Krouse 1995). The stratigraphy of the Canadian Cordillera has been studied extensively, but the deep-marine depositional environment produces regionally extensive and lithologically similar strata, creating challenges for regional and local stratigraphic correlations within the Windermere Supergroup (McMechan 2015; Smith, Arnott, and Ross 2014b). The result is a complex stratigraphic nomenclature with site specific names for correlated strata (fig. 7) (Smith, Arnott, and Ross 2014, and references therein). Within the monotonous Windermere Supergroup, the Old Fort Point Formation stands out as a distinct, widespread regional marker used to determine stratigraphic position across the southern Canadian Cordillera.

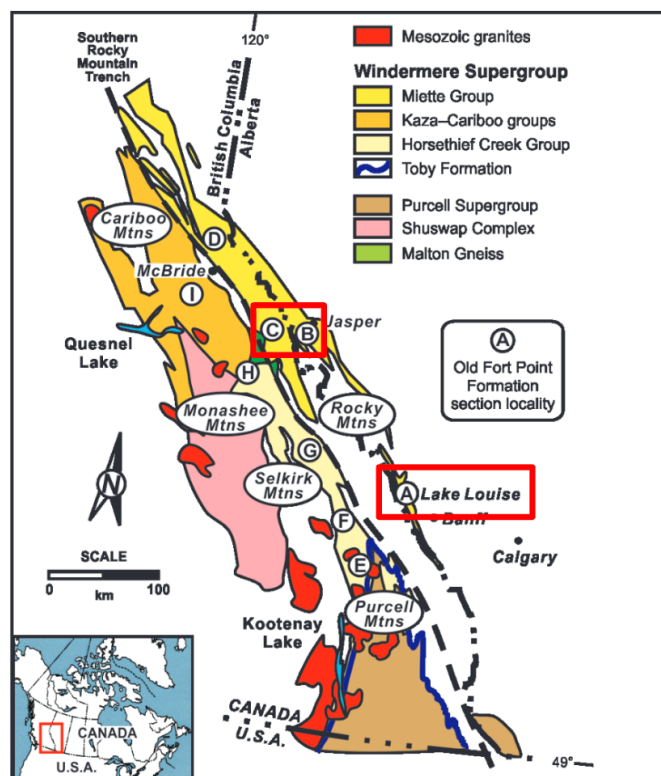


Figure 6. Simplified geologic map of the Windermere Supergroup in the southern Canadian Cordillera showing prominent outcrop localities for the OFP and correlatives. Re-Os sample locations are boxed in red. Localities: A – Lake Louise; B – Jasper National Park; C – Mount Robson Provincial Park; D – McKale River; E – Frances Creek; F – Dogtooth Range; G – Selkirk Mountains; H – Monashee Mountains; I – Cariboo Mountains. Adapted from (Smith, Arnott, and Ross 2014b).

The Old Fort Point Formation represents deep-water slope deposits of a transgressive highstand shallowing-up turbidite sequence (G. M. Ross and Murphy 1988; G. M. Ross 1991; Smith, Arnott, and Ross 2014b), and consists of three members: Temple Lake, Geikie Siding, and Whitehorn Mountain. The basal Temple Lake Member has a thickness between 50 and 125 m, and incorporates variably colored (purple, green, brown), fine-grained siltstone to mudstone with rare sandstone and limestone-siltstone couplets. The overlying Geikie Siding Member consists of 2-15 m of alternating siltstone to mudstone. The upper Whitehorn Mountain Member is the most variable, with a thickness of <.5 - 165 m, and is composed of diamictite, breccia to conglomerate, sandstone, quartzarenite, calcareous arenite, arenaceous limestone, limestone and mudstone to siltstone (Smith, Arnott, and Ross 2014b). The upper Whitehorn Mountain Member was subjected to extensive submarine canyon incision as a result of an abrupt sea level regression during regional tectonic uplift (Smith, Arnott, and Ross 2014a). The Old Fort Point Formation is overlain and underlain by various siliciclastic members of the Windermere Supergroup across the southern Canadian Cordillera.

COLUMBIA MOUNTAINS				ROCKY MOUNTAINS							
CARIBOO MOUNTAINS ¹		SELKIRK MOUNTAINS ²		PURCELL MOUNTAINS ³		SELWYN AND MAIN RANGES ⁴		JASPER ⁵		LAKE LOUISE ⁶	
Cariboo Group	Yankee Belle Fm					Upper Miette (East Twin Fm)					
	Cunningham Fm										
Kaza Group	Isaac Formation	Horsethief Group	Upper Pelite Unit	Horsethief Group	Upper Grit Division	Miette Group	Middle Miette (McKale Fm)	Miette Group	Upper Wynd Formation	Miette Group	Hector Formation
			Central Clastic Unit		Carbonate Div.				Lower Wynd Formation		
	'Marker'		Comedy Ck. Unit		Baird Brook Div.		MMM/OFP		Old Fort Point Fm		Taylor Lake/Mt. Temple mbrs
	Middle		Basal Pelite Division	Lower Grit Division	Middle Miette (McKale Fm)		Meadow Creek Formation	Corral Creek Formation			
	Lower			Basal Pelite Division & Carbonate Unit	Lower Miette (Cushing Ck. Fm)						
	Middle Marble Unit		Mid-Marble Unit	Irene Formation							
	Semipelite Amphibolite Unit		Semipelite Amphibolite Unit	Toby Formation							
	Lower Pelite Unit		Pelite Unit								

Figure 7. Stratigraphic nomenclature of the WSG in the southern Canadian Cordillera. From Smith, Arnott, and Ross 2014, and references therein.

Recent geochemical data from carbonates of the Old Fort Point Formation reveal a $\delta^{13}\text{C}$ value of $\sim -12\text{‰}$, with a carbon isotope excursion profile similar to the Shuram excursion, including a gradual recovery of $\delta^{13}\text{C}$ over the entire formation (fig. 8). Thus, the Old Fort Point Formation should correlate with regional and global Shuram excursion strata (fig. 9). In northwestern Canada, the Shuram excursion has been located in the Gametrail and Chowika Formations of the Windermere Supergroup. The age of the Gametrail is bracketed by the Re-Os ages of conformably underlying and overlying formations at 574.0 ± 4.7 Ma to 567.3 ± 3.0 Ma (fig. 9) (Rooney et al. 2020). Ages bracketing the Old Fort Point Formation roughly fit into the global age framework for the Shuram excursion. The base of the Windermere succession in the southern Canadian Cordillera is bracketed by the 728 ± 8 -7 to 740 ± 36 Ma age of nonconformably underlying granitic rocks (Parrish and Scammell 1988; Evenchick, Parrish, and Gabrielse 1984). Above the Old Fort Point Formation, the Isaac group yields an age of 567.4 ± 3.7 Ma (Boag 2020).

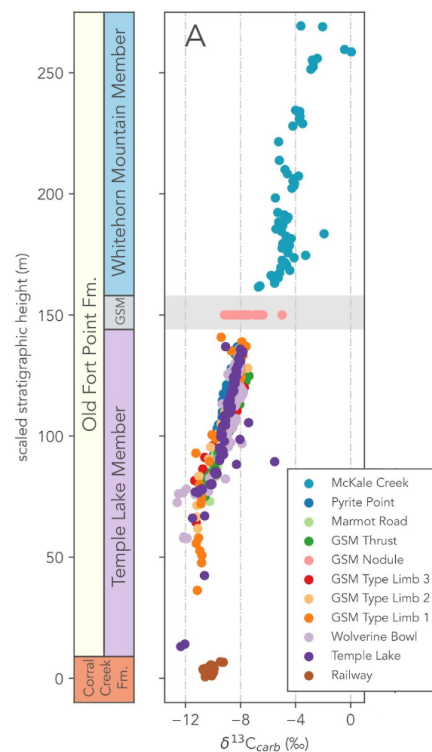


Figure 8. Compilation of $\delta^{13}\text{C}$ data from outcrops of the Old Fort Point Formation across the Southern Canadian Cordillera. Unpublished data courtesy of Connor van Wieren.

On the other hand, the Geikie Siding Member of the Old Fort Point Formation yields a Re-Os age of 607.8 ± 4.9 Ma, which does not fit within the framework of the Shuram (Kendall et al. 2004). This could indicate that the Shuram is not globally synchronous, however, the complications presented by the appearance of a Shuram-magnitude CIE 30 million years before the onset of the Shuram in other localities would have to be accounted for in any model describing the driving mechanisms of the Shuram. Since the Shuram has been shown to be synchronous in other localities, it is more likely that the Re-Os age needs to be re-evaluated with updated methods.

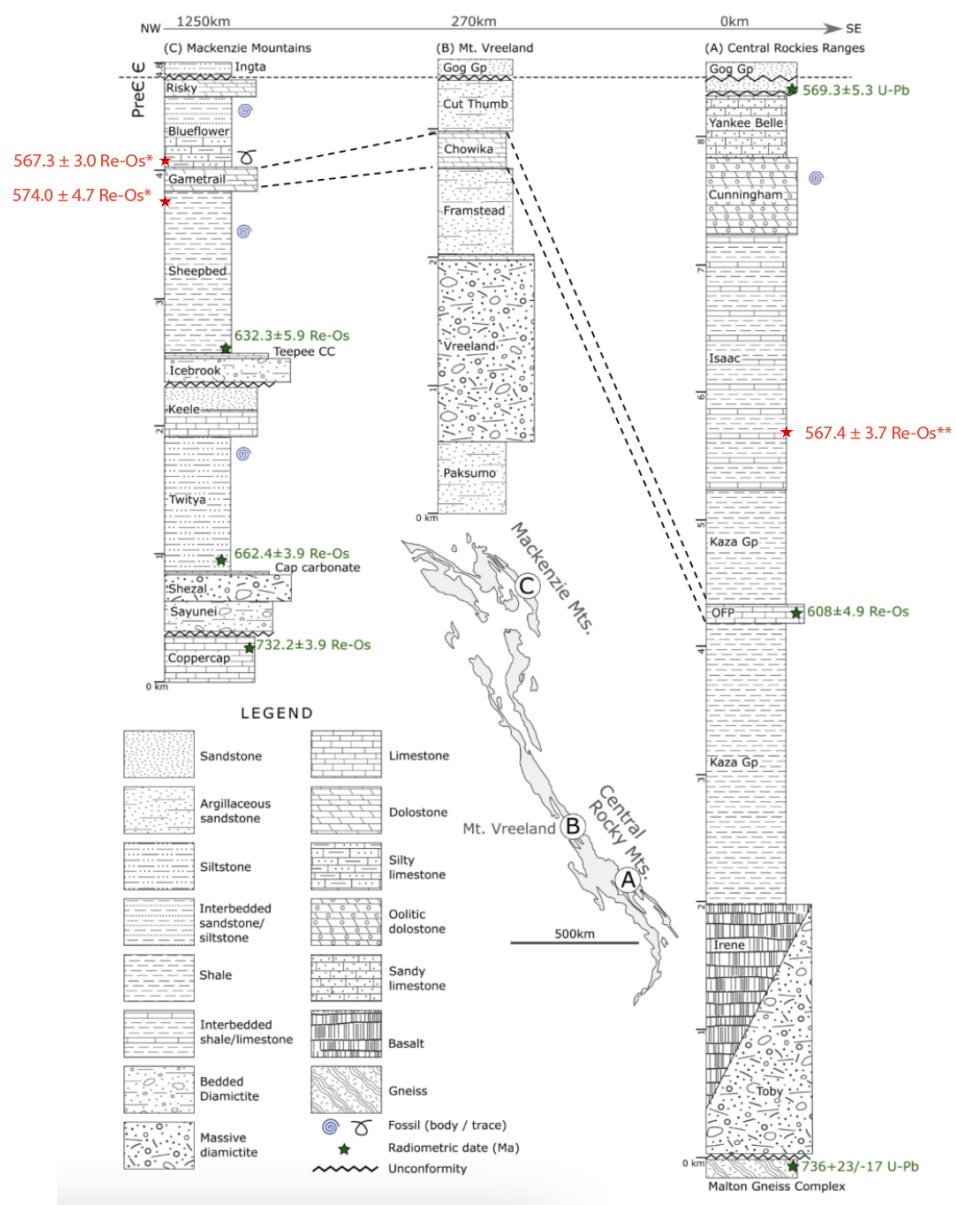


Figure 9. Stratigraphic column for the Old Fort Point Formation with dashed lines indicating potential correlation. Adapted from (Lanni 2017). (*Rooney et al. 2020; **Boag, 2020).

Samples of mudstone from the Windermere Supergroup were collected by Alan Rooney in 2022 for Re-Os isotopic analysis. Samples were taken from the Upper Miette East Twin Formation, the Old Fort Point type section, and the Temple Lake Member of the Old Fort Point Formation (fig. 10). The East Twin Formation overlies the Old Fort Point Formation in the Selwyn and Main ranges of the Canadian Rocky Mountains (fig. 7), and the sampling location is located near the Old Fort Point type section.



Figure 10. 2022 sampling locations of the Windermere Supergroup in British Columbia, Canada.

5. Methodology

5.1 Sample Preparation

Patom Supergroup samples were prepared by the author. The Imbinskaya core samples were prepared by Oren Lieber-Kotz, and samples of the Windermere Supergroup were prepared by members of the Rooney Geochronology Lab. Post-depositional surface weathering and fluid flow can result in a significant loss of Re and Os and alteration of whole rock Re-Os systematics (e.g. Peucker-Ehrenbrink and Hannigan 2000; Georgiev et al. 2012; Rooney, Chew, and Selby 2011). Rock samples were first cut using a diamond-coated rock saw to remove any weathered surfaces and then polished using a diamond-coated polishing pad to remove saw marks. Extra care was taken with Patom Supergroup samples to remove pyrite veins and inclusions. Samples were allowed to dry and then sledged using a duct-tape covered rock hammer and finely powdered ($\sim 30 \mu\text{m}$) in a zirconia ceramic ring and puck mill using a SPEX 8500 Shatterbox. A minimum of 20 g of rock powder were produced for each rock sample to ensure homogenization of Re and Os present in the sample.

5.2 Rhenium Tests

Re and Os isotopic analyses were carried out at the Yale Metal Geochemistry and Geochronology Center. Re concentration tests were performed for each sample to determine which samples had adequate Re abundance for further analysis. Approximately 0.1 g of powdered sample was digested in inverse aqua regia (3 mL $\sim 12\text{N}$ HCl and 6 mL $\sim 16\text{N}$ HNO₃) and spiked with 10 μL ¹⁸⁵Re spike solution. Samples were fluxed at $\sim 120^\circ\text{C}$ for 24-48 hours. After cooling, samples were centrifuged for 3 minutes and left to dry down overnight at 120°C .

Solvent extraction was then used to isolate Re from the digested sample. Samples were centrifuged for 3 minutes with 5 mL 5N NaOH and 5 mL acetone in order the partition Re into acetone. The Re-bearing acetone was pipetted off and evaporated at 60°C overnight. Dried samples were brought up in 4 mL 0.8N HNO₃. Re abundances were then measured on a Thermo Fisher iCAP single quadrupole inductively coupled plasma mass spectrometer (ICP-MS). In general, samples with an elemental Re abundance greater than 0.5 ppb were deemed suitable for full Re-Os geochemistry.

5.3 Re-Os Analysis

Samples with adequate Re concentration were put through full solution chemistry for Re-Os isotopic analysis using a thermal ionization mass spectrometer (TIMS). Between 0.6 and 0.9 g of sample was added to a borosilicate glass Carius tube with a known weight of ^{185}Re - ^{190}Os spike solution (~ 0.02 g) and 8-10 mL $\text{Cr}^{\text{VI}}\text{O}_3\text{-H}_2\text{SO}_4$ (chromic acid). Chromic acid digestion has been shown to preferentially liberate hydrogenous Re and Os from the rock matrix (Selby & Creaser, 2003). The mixture was frozen in a dry ice slurry to avoid volatilization of Os while sealing the Carius tube with a blowtorch. The samples were placed in steel pipe jackets and digested at 220°C for 48 hours.

Re and Os were then separated out of the digested sample by CHCl_3 (chloroform) solvent extraction. A total of 10.5 mL of chloroform was sequentially added to the sample, transferred to a centrifuge tube, and agitated using a vortex. The Os-bearing chloroform was pipetted out of the centrifuge tube and into a vial containing 3 mL 9N HBr. The sample vials were left to mix on a rocker overnight. Approximately 1 mL of the Re-bearing chromic acid was pipetted into a beaker and left to dry down overnight.

The Os-bearing HBr was then pipetted onto a watch glass covered in Teflon tape and allowed to evaporate at 80°C until ~ 20 μL were left. Each 20 μL drop was transferred to the lid of a vial, dried down on a hot plate, and stored until undergoing micro-distillation to purify the final Os cut. 20 μL of 9N HBr were added to the tip of a tristar Teflon vial. 50 μL of chromic acid were added to each dried Os cut. Tristar vials were inverted, sealed onto each lid, and heated at 80°C for 3-4 hours. During this process, Os was volatilized by the chromic acid and condensed into the HBr. The Os-bearing HBr was dried to a ~ 1 μL drop, which was loaded onto a platinum filament and coated with a $\text{Ba}(\text{OH})_2$ in 0.1 N NaOH activator solution for TIMS analysis.

Re was separated from chromic acid using NaOH-acetone solvent extraction. 15 mL of cleaned 5N NaOH was added to each dried chromic acid cut, allowed to equilibrate, added to a centrifuge tube with 15 mL acetone, and vortexed. The Re-bearing acetone was then pipetted off and evaporated overnight. Re cuts were then purified by column chromatography using 200-400

micron mesh BioRad AG1x8 anion exchange resin, dried, and loaded onto Ni filaments for isotopic analysis by TIMS.

Isotope analyses were carried out on a Thermo Fisher Triton-Plus thermal ionization mass spectrometer in negative mode (N-TIMS). Re was measured using Faraday cups in static mode as the oxides $^{185}\text{ReO}_4^-$ and $^{187}\text{ReO}_4^-$, while Os was measured as $^{186}\text{OsO}_3^-$ to $^{192}\text{OsO}_3^-$ using an electron multiplier in single collector peak-hopping mode (Robert A Creaser et al. 2002; Selby and Creaser 2003). Uncertainties were determined by propagating both internal and external errors in Re and Os mass spectrometry measurements, blank abundances and isotopic compositions, spike calibrations, and reproducibility of standard Re and Os isotopic values. The $^{187}\text{Re}/^{188}\text{Os}$ and $^{187}\text{Os}/^{188}\text{Os}$ ratios and associated uncertainties were used to create isochron regression models using the online program *IsoplotR* (Ludwig 2008).

6. Results

6.1 Rhenium Abundance

6.1.1 Patom Supergroup

Re elemental abundance for the Patom Supergroup ranged from 0 to 1.7 ppb, with the majority of samples containing less than 0.5 ppb (Table 1). These samples were therefore deemed unsuitable for Re-Os isotopic analysis.

Sample	Re (ppb)	Sample	Re (ppb)	Sample	Re (ppb)	Sample	Re (ppb)
2007-1	0.1	2020-1	0.0	2021-1	0.1	2022-1	0.6
2007-2	0.2	2020-2	0.0	2021-2	0.4	2022-2	0.1
2007-3	0.1	2020-3	0.1	2021-3	0.0	2022-3	0.0
2007-4	-0.1	2020-4	0.0	2021-4	0.3	2022-4	0.3
2007-5	0.0	2020-9	0.0	2021-5	0.2	2022-5	0.3
2007-6	0.1	2020-10	0.0	2021-6	0.2	2022-6	0.4
2007-7	0.3	2020-12	0.1	2021-7	0.3	2022-7	0.9
2007-8	0.1	2020-13	0.3	2021-8	0.0	2022-8	0.2
2007-9	0.0	2020-14	0.0	2021-9	0.1	2022-9	0.1
2007-10	0.1	2020-16	0.0	2021-10	0.1	2022-10	0.3
		2020-18	0.1	2021-11	0.1	2022-11	0.4
		2020-19	0.1	2021-13	0.1	2022-12	1.7
		2020-20	0.1	2021-14	0.1	2022-15	0.2
				2021-15	0.0		

Table 1. Re elemental abundances for Patom Supergroup samples.

6.1.2 Imbinskaya Well Core

Many samples taken from the Taseeva Group cores yielded ≥ 0.5 ppb Re. However, only one group from the Imbinskaya-3 core was chosen for Re-Os isotopic analysis before discontinuing the project. All of the samples in this group had Re abundance above 0.5 ppb (Table 2).

Sample	Re (ppb)
IZ-57/1	0.6
IZ-57/2	0.5
IZ-57/3	0.7
IZ-57/4	1.2
IZ-57/5	0.9
IZ-57/6	14.9
IZ-57/7	1.5

Table 2. Re elemental abundances for Imbinskaya-3 core samples.

6.1.3 Windermere Supergroup

All but one of the Windermere Supergroup samples yielded ≥ 0.5 ppb Re and are therefore suitable for Re-Os analysis. Samples from the A2208 horizon are from the Old Fort Point type section (fig. 10) and are significantly enriched in Re compared to other horizons. Sample horizons A2204 and A2206 are from the East Twin Formation of the Upper Miette Group, and A2209, A2210, and A2211 are from the Temple Lake Member of the Old Fort Point Formation.

Sample	Re (ppb)	Sample	Re (ppb)	Sample	Re (ppb)
A2204-A	0.9	A2206-A	0.8	A2208-A	9.8
A2204-C	0.9	A2206-B	0.6	A2208-B	11.7
A2204-D	1	A2206-C	0.9	A2208-C	10.6
A2204-G	0.7	A2206-D	0.3	A2208-D	9.1
A2204-I	0.9	A2206-E	0.9	A2208-E	7.4
		A2206-F	0.7		
		A2206-G	0.6		
		A2206-H	0.7		
		A2206-I	2.4		
A2209-A	1.8	A2210-A	1.6	A2211-A	1.6
A2209-B	1.3	A2210-B	1.8	A2211-B	1.7
A2209-C	0.9	A2210-C	1.6	A2211-C	1.6
A2209-D	1.1	A2210-D	1.8	A2211-D	1.8
A2209-E	1	A2210-E	1.6	A2211-E	1.5

A2209-F	1.2	A2210-F	1.6	A2211-F	1.2
A2209-G	1.1	A2210-G	1.8	A2211-G	1.3
A2209-H	0.9	A2210-H	2	A2211-H	1.1

Table 3. Re elemental abundances for Windermere Supergroup samples.

6.2 Re-Os Isotopic Analysis

6.2.1 Imbinskaya Well Core

Element concentrations and isotopic compositions for all of the Imbinskaya-3 samples analyzed can be found in table 4. Sample IZ-57/6 shows significant enrichment in Re compared to the other samples, as well as a lower initial $^{187}\text{Os}/^{188}\text{Os}$ ratio. With the exception of sample IZ-57/6, the initial $^{187}\text{Os}/^{188}\text{Os}$ ratios are fairly comparable. The data do not yield an isochron.

Sample	Re (ppb)	±	Os (ppt)	±	^{192}Os (ppt)	±	$^{187}\text{Re}/^{188}\text{Os}$	±	$^{187}\text{Os}/^{188}\text{Os}$	±	rho	Os i	±
IZ-57/1	0.76	0.01	61.3	0.3	21.7	0.1	69.362	1.435	1.413	0.01056	0.29006	0.64	0.02
IZ-57/2	0.52	0.01	60	0.3	21.4	0.1	48.668	1.057	1.336	0.00973	0.28312	0.79	0.02
IZ-57/3	0.93	0.02	125.1	0.5	45.9	0.2	40.338	0.785	1.0845	0.00473	0.15526	0.63	0.01
IZ-57/4	1.34	0.02	103.2	0.4	36.3	0.2	73.461	1.397	1.4535	0.00736	0.19633	0.63	0.02
IZ-57/6	13.75	0.24	158.6	1.3	25.4	0.2	1079.153	19.659	12.266	0.0788	0.2889	0.19	0.23

Table 4. Re and Os elemental concentrations and isotopic compositions for the Imbinskaya-3 core. Uncertainties are given as 2σ . Rho is the associated error correlation. Os i is the initial $^{187}\text{Os}/^{188}\text{Os}$ isotope ratio calculated at 668 Ma.

6.2.2 Windermere Supergroup

Samples from three horizons of the Windermere Supergroup have thus far been analyzed for Re and Os elemental concentrations and isotopic compositions, including two sample sets from the East Twin Formation and one from the Temple Lake Member of the Old Fort Point Formation. Samples A2204-A, C, D, H and A2206-A, C were put through Re-Os analysis twice with similar results. Data reported for these samples is from the second run. Data from all three horizons is not isochronous and gives a negative initial $^{187}\text{Os}/^{188}\text{Os}$ isotope ratio for some samples. Positive Os initial values are dissimilar for all three horizons. The Temple Lake Member is more enriched in Re and Os when compared to the East Twin Formation. In the East Twin Formation, the $^{187}\text{Os}/^{188}\text{Os}$ isotope ratio is generally higher than the modern marine average of 1.06 but lower

than the continental crust average of 1.4 (Peucker-Ehrenbrink and Ravizza 2000). The $^{187}\text{Os}/^{188}\text{Os}$ isotope ratio for the Temple Lake Member is higher than the crustal average, with an average value of 2.8.

Sample	Re (ppb)	±	Os (ppt)	±	192Os (ppt)	±	187Re/188Os	±	187Os/188Os	±	rho	Os i	±
EAST TWIN FORMATION													
A2204-A	0.55	0.00	22.9	0.1	8.1	0.0	133.3	1.0	1.368	0.009	0.708	-0.76	0.03
A2204-C	0.99	0.01	18.6	0.1	6.3	0.0	312.9	3.1	1.826	0.015	0.693	0.4	0.03
A2204-D	0.57	0.00	19.1	0.1	6.7	0.0	170.2	1.7	1.506	0.012	0.675	11.93	0.07
A2204-E	0.43	0.00	13.0	0.1	4.8	0.0	181.0	2.1	1.101	0.011	0.795	-0.63	0.02
A2204-G	3.55	0.01	12.7	0.1	4.6	0.1	1524.4	19.7	1.118	0.015	0.933	-13.43	0.19
A2204-H	0.39	0.00	20.5	0.1	7.3	0.0	106.0	1.0	1.354	0.010	0.617	0.39	0.00
EAST TWIN FORMATION													
A2206-A	0.70	0.01	16.6	0.1	6.1	0.0	227.8	2.4	1.122	0.010	0.666	-1.05	0.03
A2206-B	0.37	0.00	16.6	0.1	6.0	0.0	121.4	1.2	1.199	0.010	0.707	0.04	0.02
A2206-C	0.72	0.00	16.7	0.1	6.1	0.0	237.6	2.3	1.172	0.011	0.715	-1.09	0.02
TEMPLE LAKE MEMBER, OLD FORT POINT FORMATION													
A2210-C	2.14	0.02	58	0.3	17.8	0.1	238.8904	2.0797	2.756	0.0115	0.3423	0.477	0.02
A2210-D	1.98	0	53.2	0.3	16.2	0.1	242.9284	1.0886	2.8228	0.0126	0.7058	0.505	0.02
A2210-E	1.72	0	52.1	0.3	16	0.1	213.6408	0.9859	2.7621	0.0127	0.7054	0.724	0.02
A2210-F	2.23	0.01	52.2	0.3	15.7	0.1	282.414	1.298	2.9791	0.0131	0.719	0.284	0.02
A2210-G	7.73	0.03	57.8	0.3	17.8	0.1	862.602	4.896	2.732	0.014	0.525	-5.498	0.05
A2210-H	1.76	0	54	0.3	16.6	0.1	209.9767	0.9995	2.7282	0.0128	0.6541	0.725	0.02

Table 5. Re and Os elemental concentrations and isotopic compositions for three horizons of the Windermere Supergroup. Uncertainties are given as 2σ . Rho is the associated error correlation. Os i is the initial $^{187}\text{Os}/^{188}\text{Os}$ isotope ratio calculated at 570 Ma.

7. Discussion

7.1 Patom Supergroup

Recent Pb-Pb dating of limestones of the Bol'shoi Patom Group has confirmed an Ediacaran age for the group but has not resolved questions about its correlations with global events (Rud'ko et al. 2021). Although the Pb-Pb ages agree stratigraphically, they have large uncertainties. The base of the Barakun Formation contains a cap carbonate correlated with global cap carbonates marking the end of the Marinoan glaciation (fig. 4). If this correlation is correct, the lower Barakun Formation should have an age of ~635 Ma. Pb-Pb dating indicates a younger age of 613 ± 56 Ma (Rud'ko et al. 2021). Likewise, the upper Kalancha Formation underlies the Shuram Excursion found in the Zhuya Formation, and should therefore have an age older than the onset of the Shuram Excursion at ~575 Ma (Rooney et al. 2020). The Pb-Pb age obtained by Rud'ko et al. (2021) is slightly younger at 574 ± 16 Ma. These ages agree with stratigraphic correlation within uncertainty, but precise Re-Os ages for all of these formations would greatly aid in evaluating relationships between characteristics of the Patom Supergroup, including the C-isotope record, Marinoan glaciation associated strata, and the appearance of micro- and macrofossils.

The studied samples were not enriched enough in Re to be viable for Re-Os isotopic analysis (Table 1). This may have resulted either from an original lack of ^{187}Re in the sampled lithology, or from post-depositional addition or loss of Re or Os. Re and Os are mobile and therefore lost during oxidative weathering, disturbing the Re-Os isochron (Georgiev et al. 2012). The Patom Supergroup samples showed signs of surficial weathering, including pyrite veins and weathered surfaces within fissures in the rocks. A few samples consisted only of thin shards and flakes of shale. This indicates that the samples were improperly taken for Re-Os analysis.

7.2 Taseeva Group

Despite a lack of definitive age constraints on the Taseeva Group of southwestern Siberia, the group is likely Ediacaran based on litho- and chemostratigraphic correlation with the Zhuya Group within the Patom basin. The Chistyakova Formation exhibits a Shuram-correlative CIE with a nadir of -13‰ (Kochnev et al. 2020). Maximum depositional ages obtained from detrital

zircons are consistent with an Ediacaran age for the Taseeva Group, but fall short of confirming a relationship between the Chistyakova Formation and global Shuram excursion correlates. Re-Os dates would provide key context for evaluating the geochemical and biological characteristics of the Taseeva Group.

Due to developing geopolitical events, the Taseeva Group drillcore samples lack essential stratigraphic information, rendering any age constraints obtained for the samples difficult to interpret. The project was discontinued for this reason. However, further analysis of the Taseeva drillcores is likely to yield isochronous data. Initial Re-Os analysis of the Imbinskaya core shows that Re and Os are sufficiently enriched, and initial Os isotopic composition is fairly uniform (Table 4).

7.3 Windermere Supergroup

Recent data and a re-evaluation of the stratigraphy of the Old Fort Point Formation suggests that it correlates with regional strata representing the Shuram negative carbon isotope excursion. Carbon isotope data from the formation suggest that the $\delta^{13}\text{C}$ nadir is about -12‰, matching the magnitude of the Shuram excursion. Lithologically, the Old Fort Point Formation is aligned with features found in global Shuram strata, including the presence of large submarine canyon incisions within the uppermost part of the Shuram strata (Grotzinger, Fike, and Fischer 2011; Smith, Arnott, and Ross 2014b). However, a Re-Os analysis yielded an age of 607.8 ± 4.9 Ma, which is outside the known geochronological bounds of the Shuram excursion (Kendall et al. 2004; Rooney et al. 2020). This warrants a re-evaluation of the age model for this formation. As there have been improvements in Re-Os analysis methods since the 2004 age was obtained, we hypothesize that reinvestigating the Old Fort Point Formation will yield an age within the bounds of the Shuram excursion (574.0 ± 4.7 and 567.3 ± 3.0 Ma) (Rooney et al. 2020).

Samples from three horizons of the Windermere Supergroup have thus far been analyzed. Although the samples are sufficiently enriched in Re for Re-Os analysis (Table 3), the data do not yield an isochron. The samples may have been subjected to surficial weathering, altering Re-Os systematics. It may be possible to obtain an isochron from the current samples with further analysis.

8. Conclusions and Future Work

The Neoproterozoic Era was a dynamic period of Earth's history and recorded fluctuations in Earth systems, including Snowball Earth glaciations and the Shuram carbon isotope excursion. Although these events have been detected in strata globally, a lack of age constraints have led to controversy over their timing, duration, drivers, and role in environmental and ecological developments. Constraining their onset, termination and duration in several locations would inform models of their driving mechanisms and effects on Earth systems. The Re-Os isotope system provides an opportunity to obtain precise ages for sedimentary strata, although the rocks must be sufficiently enriched in Re and have similar Os initial isotopic compositions in order to yield an isochron. Re-Os analysis of samples from Siberia and British Columbia proved difficult. Samples from the Taseeva Group and Windermere Supergroup will continue to be analyzed in the coming year.

9. Acknowledgments

I would like to thank my advisor, Alan Rooney, for his guidance, expertise, and support throughout the duration of this project. I am also grateful to Sam Shipman, for his mentorship, patience, and guidance in the laboratory, and for his willingness to share his knowledge. I would also like to thank Sierra Anseeuw for her help in learning lab methods. Thank you to Jordan Wostbrock for her time in serving as second reader. Lastly, thank you to DUS Mary-Louise Timmermans and DUS Celli Hull for their encouragement and advice throughout my time at Yale.

10. References

- Boag, Thomas H, James F Busch, Zachary T Sickmann, Jack C Taylor, James L Crowley, Justin V Strauss, and Erik A Sperling. 2020. “Carbon Isotope Chemostratigraphic Correlation Of The Windermere Supergroup, British Columbia, Canada.”
- Boag, Thomas Howard. 2020. “The Role of Ecophysiology and Paleoenvironmental Dynamics in the Ediacaran Biostratigraphic Record.” Ph.D., United States -- California: Stanford University.
<https://www.proquest.com/docview/2734696912/abstract/6639982327314141PQ/1>.
- Busch, James F., Eben B. Hodgin, Anne-Sofie C. Ahm, Jon M. Husson, Francis A. Macdonald, Kristin D. Bergmann, John A. Higgins, and Justin V. Strauss. 2022. “Global and Local Drivers of the Ediacaran Shuram Carbon Isotope Excursion.” *Earth and Planetary Science Letters* 579 (February): 117368. <https://doi.org/10.1016/j.epsl.2022.117368>.
- Chumakov, N. M., I. N. Kapitonov, M. A. Semikhatov, M. V. Leonov, and S. V. Rud’ko. 2011. “Vendian Age of the Upper Part of the Patom Complex in Middle Siberia: U/Pb LA-ICPMS Dates of Detrital Zircons from the Nikol’skoe and Zherba Formations.” *Stratigraphy and Geological Correlation* 19 (2): 233–37.
<http://dx.doi.org/10.1134/S0869593811020043>.
- Chumakov, N. M., M. A. Semikhatov, and V. N. Sergeev. 2013. “Vendian Reference Section of Southern Middle Siberia.” *Stratigraphy and Geological Correlation* 21 (4): 359–82.

<https://doi.org/10.1134/S0869593813040023>.

Cohen, Anthony S, Angela L Coe, Jessica M Bartlett, and Chris J Hawkesworth. 1999. "Precise Re–Os Ages of Organic-Rich Mudrocks and the Os Isotope Composition of Jurassic Seawater." *Earth and Planetary Science Letters* 167 (3): 159–73.

[https://doi.org/10.1016/S0012-821X\(99\)00026-6](https://doi.org/10.1016/S0012-821X(99)00026-6).

Creaser, R. A., D. A. Papanastassiou, and G. J. Wasserburg. 1991. "Negative Thermal Ion Mass Spectrometry of Osmium, Rhenium and Iridium." *Geochimica et Cosmochimica Acta* 55 (1): 397–401. [https://doi.org/10.1016/0016-7037\(91\)90427-7](https://doi.org/10.1016/0016-7037(91)90427-7).

Creaser, Robert A, Poulomi Sannigrahi, Thomas Chacko, and David Selby. 2002. "Further Evaluation of the Re-Os Geochronometer in Organic-Rich Sedimentary Rocks: A Test of Hydrocarbon Maturation Effects in the Exshaw Formation, Western Canada Sedimentary Basin." *Geochimica et Cosmochimica Acta* 66 (19): 3441–52.

[https://doi.org/10.1016/S0016-7037\(02\)00939-0](https://doi.org/10.1016/S0016-7037(02)00939-0).

Erwin, Douglas H., Marc Laflamme, Sarah M. Tweedt, Erik A. Sperling, Davide Pisani, and Kevin J. Peterson. 2011. "The Cambrian Conundrum: Early Divergence and Later Ecological Success in the Early History of Animals." *Science* 334 (6059): 1091–97.

<https://doi.org/10.1126/science.1206375>.

Evenchick, Carol, R. R. Parrish, and Hubert Gabrielse. 1984. "Precambrian Gneiss and Late Proterozoic Sedimentation in North-Central British Columbia | Geology | GeoScienceWorld."

<https://pubs.geoscienceworld.org/gsa/geology/article/12/4/233/203669/Precambrian-gneiss-and-late-Proterozoic>.

Fike, D. A., J. P. Grotzinger, L. M. Pratt, and R. E. Summons. 2006. "Oxidation of the Ediacaran Ocean." *Nature* 444 (7120): 744–47. <https://doi.org/10.1038/nature05345>.

Georgiev, Svetoslav, Holly J. Stein, Judith L. Hannah, Hermann M. Weiss, Bernard Bingen, Guangping Xu, Elin Rein, et al. 2012. "Chemical Signals for Oxidative Weathering Predict Re–Os Isochronicity in Black Shales, East Greenland." *Chemical Geology*, Special Issue Recent Advances in Trace Metal Applications to Paleoceanographic

- Studies, 324–325 (September): 108–21. <https://doi.org/10.1016/j.chemgeo.2012.01.003>.
- Grotzinger, John P., David A. Fike, and Woodward W. Fischer. 2011. “Enigmatic Origin of the Largest-Known Carbon Isotope Excursion in Earth’s History.” *Nature Geoscience* 4 (5): 285–92. <https://doi.org/10.1038/ngeo1138>.
- Halverson, Galen P., Paul F. Hoffman, Daniel P. Schrag, Adam C. Maloof, and A. Hugh N. Rice. 2005. “Toward a Neoproterozoic Composite Carbon-Isotope Record.” *GSA Bulletin* 117 (9–10): 1181–1207. <https://doi.org/10.1130/B25630.1>.
- Hoffman, Paul F., Dorian S. Abbot, Yosef Ashkenazy, Douglas I. Benn, Jochen J. Brocks, Phoebe A. Cohen, Grant M. Cox, et al. 2017. “Snowball Earth Climate Dynamics and Cryogenian Geology-Geobiology.” *Science Advances* 3 (11): e1600983. <https://doi.org/10.1126/sciadv.1600983>.
- James, Noel P., Guy M. Narbonne, and T. Kurtis Kyser. 2001. “Late Neoproterozoic Cap Carbonates: Mackenzie Mountains, Northwestern Canada: Precipitation and Global Glacial Meltdown.” *Canadian Journal of Earth Sciences* 38 (8): 1229–62. <https://doi.org/10.1139/e01-046>.
- Kaufman, Alan J., Andrew H. Knoll, and Guy M. Narbonne. 1997. “Isotopes, Ice Ages, and Terminal Proterozoic Earth History.” *Proceedings of the National Academy of Sciences* 94 (13): 6600–6605. <https://doi.org/10.1073/pnas.94.13.6600>.
- Kendall, Brian S., Robert A. Creaser, Gerald M. Ross, and David Selby. 2004. “Constraints on the Timing of Marinoan ‘Snowball Earth’ Glaciation by 187Re–187Os Dating of a Neoproterozoic, Post-Glacial Black Shale in Western Canada.” *Earth and Planetary Science Letters* 222 (3): 729–40. <https://doi.org/10.1016/j.epsl.2004.04.004>.
- Kirschvink, Joseph L. 1992. “Late Proterozoic Low-Latitude Global Glaciation: The Snowball Earth.” In , edited by J. William Schopf and Cornelis Klein, 51–52. New York: Cambridge University Press. <https://resolver.caltech.edu/CaltechAUTHORS:20130117-100718783>.
- Knoll, A. H., J. M. Hayes, A. J. Kaufman, K. Swett, and I. B. Lambert. 1986. “Secular Variation

- in Carbon Isotope Ratios from Upper Proterozoic Successions of Svalbard and East Greenland.” *Nature* 321 (6073): 832–38. <https://doi.org/10.1038/321832a0>.
- Kochnev, B.B., A.I. Proshenkin, B.G. Pokrovsky, and E.F. Letnikova. 2020. “Vendian Taseeva Group, Southwestern Margin of the Siberian Platform: Isotope, Geochemical, and Geochronological Data, Age, and Correlation.” *Russian Geology and Geophysics* 61 (10): 1121–35. <https://doi.org/10.15372/RGG2019142>.
- Lanni, Jordan. 2017. “Old Fort Point Formation: Neoproterozoic Negative D13C Excursion Recorded in a DeepWater Carbonate Succession.” *UC Riverside Electronic Theses and Dissertations*.
<https://escholarship.org/content/qt2hw6n1pj/qt2hw6n1pj.pdf?t=ozicf5&v=lg>.
- Liu, Alexander, Martin Brasier, Olga K. Bogolepova, Elena Raevskaya, and Alexander Gubanov. 2013. “First Report of a Newly Discovered Ediacaran Biota from the Irkineeva Uplift, East Siberia,” August.
- Ludwig, K. 2008. “Isoplot Version 4.15: A Geochronological Toolkit for Microsoft Excel.” *Berkeley Geochronology Center Special Publication* 4: 247–70.
- McMechan, M.E. 2015. “The Neoproterozoic Succession of the Central Rocky Mountains, Canada.” *Bulletin of Canadian Petroleum Geology* 63 (3): 243–73.
<https://doi.org/10.2113/gscpgbull.63.3.243>.
- Meert, Joseph G., and Bruce S. Lieberman. 2008. “The Neoproterozoic Assembly of Gondwana and Its Relationship to the Ediacaran–Cambrian Radiation.” *Gondwana Research, Snowball Earth to Cambrian Explosion*, 14 (1): 5–21.
<https://doi.org/10.1016/j.gr.2007.06.007>.
- Melezhik, V. A. 2009. “Constraints on $^{87}\text{Sr}/^{86}\text{Sr}$ of Late Ediacaran Seawater: Insight from Siberian High-Sr Limestones | Journal of the Geological Society | GeoScienceWorld.”
<https://pubs.geoscienceworld.org/jgs/article/166/1/183/372651/Constraints-on-87Sr-86Sr-of-Late-Ediacaran>.
- Metelkin, D.V., V.A. Vernikovskiy, and A.Yu. Kazansky. 2012. “Tectonic Evolution of the

- Siberian Palecontinent from the Neoproterozoic to the Late Mesozoic: Paleomagnetic Record and Reconstructions.” *Russian Geology and Geophysics* 53 (7): 675–88.
<https://doi.org/10.1016/j.rgg.2012.05.006>.
- Narbonne, G.M., S. Xiao, G.A. Shields, and J.G. Gehling. 2012. “The Ediacaran Period.” In *The Geologic Time Scale*, 413–35. Elsevier.
<https://doi.org/10.1016/B978-0-444-59425-9.00018-4>.
- Parrish, R. R., and R. J. Scammell. 1988. “Gneiss and Its Metamorphic Zircons, Monashee Complex, Southeastern British Columbia; Radiogenic Age and Isotopic Studies: Report 2.” Geological Survey of Canada Paper 1988-2.
- Peucker-Ehrenbrink, B., and G. Ravizza. 2000. “The Marine Osmium Isotope Record.” *Terra Nova* 12 (5): 205–19. <https://doi.org/10.1046/j.1365-3121.2000.00295.x>.
- Peucker-Ehrenbrink, Bernhard, and Robyn Hannigan. 2000. “Effects of Black Shale Weathering on the Mobility of Rhenium and Platinum Group Elements | Geology | GeoScienceWorld.”
<https://pubs.geoscienceworld.org/gsa/geology/article/28/5/475/188554/Effects-of-black-shale-weathering-on-the-mobility>.
- Pokrovsky, B. G., N. M. Chumakov, V. A. Melezhik, and M. I. Bujakaite. 2010. “Geochemical Properties of Neoproterozoic ‘Cap Dolomites’ in the Patom Paleobasin and Problem of Their Genesis | SpringerLink,” November.
<https://link.springer.com/article/10.1134/S0024490210060052>.
- Pokrovsky, B. G., V. A. Melezhik, and M. I. Bujakaite. 2006. “Carbon, Oxygen, Strontium, and Sulfur Isotopic Compositions in Late Precambrian Rocks of the Patom Complex, Central Siberia: Communication 1. Results, Isotope Stratigraphy, and Dating Problems.” *Lithology and Mineral Resources* 41 (5): 450–74.
<https://doi.org/10.1134/S0024490206050063>.
- Powerman, Vladislav, Andrey Shatsillo, Nikolai Chumakov, Igor Kapitonov, and Jeremy Hourigan. 2015. “Interaction between the Central Asian Orogenic Belt (CAOB) and the Siberian Craton as Recorded by Detrital Zircon Suites from Transbaikalia.” *Precambrian*

- Research* 267 (September): 39–71. <https://doi.org/10.1016/j.precamres.2015.05.015>.
- Priyatkina, Nadezhda, William J. Collins, Andrei K. Khudoley, Elena F. Letnikova, and Hui-Qing Huang. 2018. “The Neoproterozoic Evolution of the Western Siberian Craton Margin: U-Pb-Hf Isotopic Records of Detrital Zircons from the Yenisey Ridge and the Prisayan Uplift.” *Precambrian Research* 305 (February): 197–217. <https://doi.org/10.1016/j.precamres.2017.12.014>.
- Ravizza, Greg, and Karl K. Turekian. 1989. “Application of the ^{187}Re - ^{187}Os System to Black Shale Geochronometry.” *Geochimica et Cosmochimica Acta* 53 (12): 3257–62. [https://doi.org/10.1016/0016-7037\(89\)90105-1](https://doi.org/10.1016/0016-7037(89)90105-1).
- Rooney, Alan D., Marjorie D. Cantine, Kristin D. Bergmann, Irene Gómez-Pérez, Badar Al Baloushi, Thomas H. Boag, James F. Busch, Erik A. Sperling, and Justin V. Strauss. 2020. “Calibrating the Coevolution of Ediacaran Life and Environment.” *Proceedings of the National Academy of Sciences* 117 (29): 16824–30. <https://doi.org/10.1073/pnas.2002918117>.
- Rooney, Alan D., David M. Chew, and David Selby. 2011. “Re–Os Geochronology of the Neoproterozoic–Cambrian Dalradian Supergroup of Scotland and Ireland: Implications for Neoproterozoic Stratigraphy, Glaciations and Re–Os Systematics.” *Precambrian Research* 185 (3): 202–14. <https://doi.org/10.1016/j.precamres.2011.01.009>.
- Rooney, Alan D., Francis A. Macdonald, Justin V. Strauss, Francis Dudas, Christian Hallmann, and David Selby. 2014. “Re-Os Geochronology and Coupled Os-Sr Isotope Constraints on the Sturtian Snowball Earth.” <https://www.pnas.org/doi/10.1073/pnas.1317266110>.
- Ross, G. M. 1991. “Tectonic Setting of the Windermere Supergroup Revisited.” *Geology* 19 (11): 1125. [https://doi.org/10.1130/0091-7613\(1991\)019<1125:TSOTWS>2.3.CO;2](https://doi.org/10.1130/0091-7613(1991)019<1125:TSOTWS>2.3.CO;2).
- Ross, G. M., and D. C. Murphy. 1988. “Transgressive Stratigraphy, Anoxia, and Regional Correlations Within the Late Precambrian Windermere Grit Of the Southern Canadian Cordillera.” *Geology* 16 (2): 139–43. [https://doi.org/10.1130/0091-7613\(1988\)016<0139:TSAARC>2.3.CO;2](https://doi.org/10.1130/0091-7613(1988)016<0139:TSAARC>2.3.CO;2).

- Ross, Gerald M., John D. Bloch, and H. Roy Krouse. 1995. "Neoproterozoic Strata of the Southern Canadian Cordillera and the Isotopic Evolution of Seawater Sulfate." *Precambrian Research*, Neoproterozoic Stratigraphy and Earth History, 73 (1): 71–99. [https://doi.org/10.1016/0301-9268\(94\)00072-Y](https://doi.org/10.1016/0301-9268(94)00072-Y).
- Rud'ko, Sergey V., Anton B. Kuznetsov, Peter Yu. Petrov, Daria R. Sitkina, and Olga K. Kaurova. 2021. "Pb-Pb Dating of the Dal'nyaya Taiga Group in the Ura Uplift of Southern Siberia: Implications for Correlation of C-Isotopic and Biotic Events in the Ediacaran." *Precambrian Research* 362 (May). <https://doi.org/10.1016/j.precamres.2021.106285>.
- Saltzman, M.R., and E. Thomas. 2012. "Carbon Isotope Stratigraphy." In *The Geologic Time Scale*, 207–32. Elsevier. <https://doi.org/10.1016/B978-0-444-59425-9.00011-1>.
- Schidlowski, Manfred, and Paul Aharon. 1992. "Carbon Cycle and Carbon Isotope Record: Geochemical Impact of Life over 3.8 Ga of Earth History." In *Early Organic Evolution*, edited by Manfred Schidlowski, Stjepko Golubic, Michael M. Kimberley, David M. McKirdy, and Philip A. Trudinger, 147–75. Berlin, Heidelberg: Springer Berlin Heidelberg. https://doi.org/10.1007/978-3-642-76884-2_11.
- Selby, David, and Robert A. Creaser. 2003. "Re–Os Geochronology of Organic Rich Sediments: An Evaluation of Organic Matter Analysis Methods." *Chemical Geology* 200 (3): 225–40. [https://doi.org/10.1016/S0009-2541\(03\)00199-2](https://doi.org/10.1016/S0009-2541(03)00199-2).
- Shirey, Steven B., and Richard J. Walker. 1998. "The Re-Os Isotope System in Cosmochemistry and High-Temperature Geochemistry." *Annual Review of Earth and Planetary Sciences* 26: 423.
- Smith, M. D., R. W. C. Arnott, and G. M. Ross. 2014a. "Physical and Geochemical Controls on Sedimentation along an Ancient Continental Margin: The Deep-Marine Old Fort Point Formation (Ediacaran), Southern Canadian Cordillera." *Bulletin of Canadian Petroleum Geology* 62 (1): 14–36. <https://doi.org/10.2113/gscpgbull.62.1.14>.
- . 2014b. "The Old Fort Point Formation: Redefinition and Formal Subdivision of a Distinctive Stratigraphic Marker in the Neoproterozoic Windermere Supergroup,

Southern Canadian Cordillera.” *Bulletin of Canadian Petroleum Geology* 62 (1): 1–13.
<https://doi.org/10.2113/gscpgbull.62.1.1>.

Sobolev, Bredikhin, Merkulov, and Orekhov. 2015. “Features of processing and interpretation of magnetic and lithochemical data while exploring oil and gas fields in Siberian platform conditions (by the example of Imbinskaya gas-bearing area).” *BULLETIN OF THE TOMSK POLYTECHNIC UNIVERSITY*.

Vorob’eva, N. G., and P. Yu. Petrov. 2020. “Microbiota of the Barakun Formation and Biostratigraphic Characteristics of the Dal’nyaya Taiga Group: Early Vendian of the Ural Uplift (Eastern Siberia).” *Stratigraphy and Geological Correlation* 28 (4): 365–80.
<https://doi.org/10.1134/S0869593820040103>.